Heat transfer augmentation in 3D internally finned and microfinned helical tube

Longjian Li [a], Wenzhi Cui [a], Quan Liao [a], Xin Mingdao [a],
Tien-Chien Jen [b,*], Qinghua Chen [b]

[a] *College of Power Engineering, Chongqing University, Chongqing 400044, China*
[b] *Department of Mechanical Engineering, University of Wisconsin, Milwaukee, WI 53211, USA*

Abstract

Experiments are performed to investigate the single-phase flow and flow-boiling heat transfer augmentation in 3D internally finned and micro-finned helical tubes. The tests for single-phase flow heat transfer augmentation are carried out in helical tubes with a curvature of 0.0663 and a length of 1.15 m, and the examined range of the Reynolds number varies from 1000 to 8500. Within the applied range of Reynolds number, compared with the smooth helical tube, the average heat transfer augmentation ratio for the two finned tubes is 71% and 103%, but associated with a flow resistance increase of 90% and 140%, respectively. A higher fin height gives a higher heat transfer rate and a larger friction flow resistance. The tests for flow-boiling heat transfer are carried out in 3D internally micro-finned helical tube with a curvature of 0.0605 and a length of 0.668 m. Compared with that in the smooth helical tube, the boiling heat transfer coefficient in the 3D internally micro-finned helical tube is increased by 40–120% under varied mass flow rate and wall heat flux conditions, meanwhile, the flow resistance is increased by 18–119%, respectively.
© 2005 Elsevier Ltd. All rights reserved.

Keywords: Helical tube; Finned tube; Convective heat transfer; Boiling heat transfer

1. Introduction

Because helical tube heat exchanger has the same good characteristics as the commonly used shell-tube heat exchanger, e.g., strong structure, good adaptability, easy manufacturing and low cost, it has been widely used in many industrial applications, such as air condi-tioning, refrigeration, chemical engineering industry and pharmaceutical applications. As the past researches have shown, the secondary flow in the helical tube played an important role for the heat transfer enhancement in the laminar flow regime. Compared with the straight tube, the heat transfer augmentation ratio of single-phase flow was up to 2.0–4.0 for laminar flow and only 1.1–1.3 for turbulent flow [1–3]. However, for many applications, the heat transfer process involving the helical tube may not be of single-phase flow only, but of two-phase flow as well. The experimental results of the flow boiling heat transfer in helical tube have shown that the average heat transfer coefficient

---

* Corresponding author. Tel.: +1 414 229 2307; fax: +1 414 229 6958.
E-mail address: jen@cae.uwm.edu (T.-C. Jen).

Nomenclature

C_p	specific heat, kJ/kg °C	P_c	circumferential pitch of the internal fins, mm
d_i	helical internal diameter, m	Q_{test}	power on the helical testing tube, W
D_c	diameter of coil, m	q	heat flux, W/m^2
D_n	Dean number [$= Re \cdot \delta^{1/2}$]	r	latent heat, kJ/kg
e	fin height, m	Re	Reynolds number $\left[= \frac{\rho \cdot u \cdot d_i}{\mu}\right]$
f_c	flow resistance factor [$= \tau_w/(\rho u^2/2)$]		
F	heat transfer area, m^2	t_{wi}	temperature of the inside wall of the helical testing tube, °C
G	mass flux, kg/(m^2.s)		
h	heat transfer coefficient $\left[= \frac{Q_{test}}{F \cdot (t_{wi} - t_s)}\right]$	t_s	saturated temperature of refrigerant, °C
$\bar{h}$	integrated average heat transfer coefficient $\left[= \frac{\int_{x_1}^{x_2} h\,dx}{x_2 - x_1}\right]$	t_{pre}	refrigerant temperature in the pre-heater, °C
		W	upper width of the fin, mm
		x	mass quality $\left[= \frac{Q_{pre} - m \cdot C_p \cdot (t_s - t_{pre})}{m \cdot r}\right]$
Nu	Nusselt number $\left[= \frac{h \cdot d_k}{\lambda}\right]$		
		Greek symbols	
p	Pressure, Pa	δ	curvature of the helical tube [$= d_i/D_c$]
P_a	axial pitch of the internal finned tube, mm	ρ	density, kg/m^3

increased by only 5–15% compared with the straight tube flow boiling cases [4].

It has been believed, in most cases, that the heat transfer step at the internal side of the helical tube was the bottleneck of the overall performance of the heat exchanger. Therefore, it has been proposed in this paper to enhance the heat transfer rate in the internal side of the helical tube. It is worth noting that internally finned surface enhancement method can be directly applied to helical tube with both single-phase flow and two-phase flow (boiling).

In the case of single-phase flow the 3D internal fins have been applied in straight tube to enhance the convective heat transfer component and the experimental results with air flow by Liao et al. [5] have shown that the augmentation ratio of heat transfer varied from 2.5 to 3.5 with the Reynolds number ranging from 4000 to 25,000. On the other side, the flow-boiling heat transfer characteristics have been extensively investigated for micro-finned straight tubes with single helix geometry (so-called 2D micro-finned tubes), and as reviewed by Bergles [6], the heat transfer enhancement ratio of this kind of tube can be up to 2.0. Chamra and Webb [7] compared the flow boiling heat transfer performance of a 3D micro-finned straight tube, which has cross-grooves geometry, with 2D micro-finned tube. Their results showed that the new geometry 3D micro-finned tube could provide a heat transfer coefficient 31% higher than the 2D micro-finned tube.

So far, there have been no reports in the literature for the heat transfer augmentation in the internal side of the helical tube with extended surface. Therefore, the major purpose of this research is to investigate the heat transfer improvement and flow resistance characteristics with a new 3D internally finned helical tube both in single-phase flow and in two-phase (boiling) flow regimes. It has been well known that the 3D internally finned surface for heat transfer enhancement was first applied in straight tube and the increase in heat transfer rate in single-phase flow was significantly better than those of other enhancement methods, such as 2D rough surface, embedded thread, twisted belt and so on. For the two-phase (boiling) flow, the unique structure of 3D micro-fins can significantly increase the number of the nucleate boiling sites and therefore greatly enhances the heat transfer rate; meanwhile, it has been found that the increase of the pressure drop was very small.

Therefore, if the 3D internally finned surface enhancement combines with the inherent helical tube's strong secondary flow characteristic, the increase in heat transfer rate of the helical tube heat exchanger could be greatly improved and thus the size of the heat exchanger may become smaller. This new type of helical tube can present a new breakthrough in the heat transfer performance against the common smooth helical tube. This paper describes the experimental study conducted for the 3D internally finned helical tube, and the findings in this study not only will advance the development of high efficiency heat exchangers, but also can be used to other engineering applications, such as pharmaceutical applications, refrigeration, chemical engineering industry and so on.

2. Experimental scheme

The experimental scheme for single-phase flow is shown in Fig. 1. For the both experimental systems, the experiments are carried out in the room temperature (about 27.0 °C). The tested helical copper tube has an
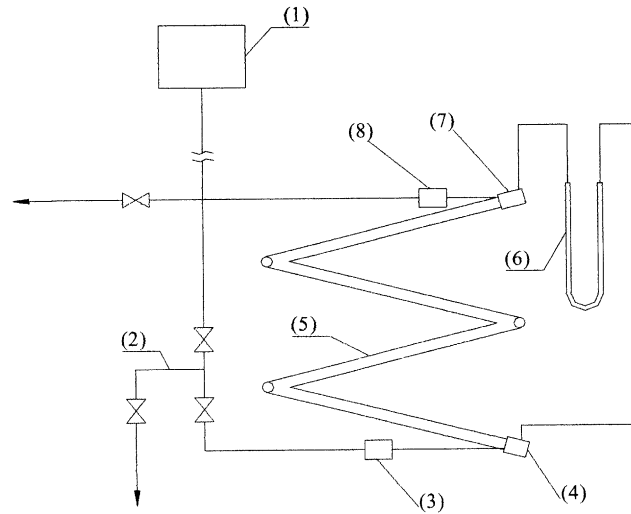
Fig. 1. Schematics of the single-phase flow experiment. (1) Tank; (2) by pass tube; (3) water inlet chamber; (4) gauge ring; (5) helical tube; (6) pressure gauge; (7) gauge ring; (8) water outlet chamber.

outer diameter of 16.0 mm, thickness of 2.0 mm, a helical internal diameter of 181.0 mm, a helical pitch of 75.0 mm, and is made of two loop systems (working fluid loop and cooling water loop). The working substances are water and refrigerant R134a for single-phase and two-phase experiments, respectively. For the cooling water, its inlet temperature was measured to be about 22.0 °C. For the working medium, its temperature depends on the different experimental conditions, but the temperature range was between 15.0 °C and

35.0 °C. After many experiments and numerical analyses in the whole laminar flow regime, Manlapaz & Churchill et al. [3] had concluded that the heat transfer increase in smooth helical tube was remarkably influenced by the gravity when the helical pitch is larger than the helical diameter. Based on that conclusion, the helical tube used in this experimental study was purposely close to a horizontal coiled tube with a helical pitch of 75.0 mm; and a helical diameter of 181.0 mm. The tested helical tube with a total length of 1147.0 mm has a straight stable
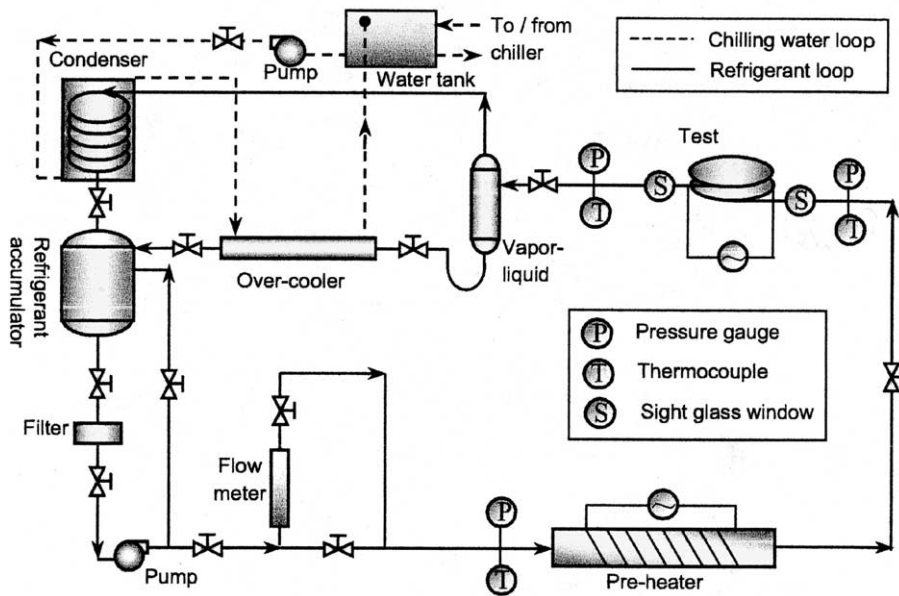

Fig. 2. Schematics of two-phase flow experiment.

flow part of 500.0 mm length, which is located at the inlet of the test section. In order to supply the test section with uniform heat flux, a flat band heater (whose cross section is 4×0.2 mm) is closely placed and tightly wrapped around the outer surface of the testing tubes. An electric transformer is used in these experiments to adjust the heat flux by varying the power inputs. When both the voltage at the ends of the band heater and current are measured, the power, which is added on the outer surface of helical testing tube, can be calculated directly. To decrease the heat loss to the environment, a thermally-insulating material (glass fiber mat), whose thermal conductivity is 0.043 W/(m K), is wrapped on the outer surface of the helical testing tubes with a thickness of 30.0 mm. Before each experiment, an energy balance experiment is conducted and the result demonstrated that the heat loss to the environment is within 5.0% on condition that the test temperature is below 35.0 °C. The effect of heat loss has been accounted for all the data obtained from the experiments. Since in this experiment the temperature is the key parameter that needs to be measured accurately, calibrated thermocouples mounted on the outer surface of the helical testing tubes' wall are used as temperature sensors. In order to monitor the temperature distribution around the cross section of the helical testing tube, four pairs of thermocouples, which are uniformly located around the cross section of testing tube, are mounted on the outer surface of the middle and near the outlet of the helical testing tubes, respectively. The locations of thermocouple are shown in Fig. 3. To know the temperature variations along the helical axis, additional six sets (each one includes four pairs of thermocouples) of thermocouples are uniformly placed on the outer surface of the helical testing tube. The temperatures of the inlet and outlet cooling water are measured at their chambers by three thermocouples, respectively. For the measurement of working fluid pressure drop along the test sections in the experiments a simple, but reliable and precise U-type manometer method is used to directly display the pressure difference between the inlet and outlet of the experimental test section. The uncertainty of the pressure drop in the experiment using this method is ±133.0 Pa. Meanwhile a valve is used to control the cooling water's mass flow rate. In order to achieve stable flow for the cooling water, a tank, which is placed 10 m above the helical testing tube, is used in these experiments. Finally, all of the thermocouples are linked to the data acquisition system (HP3457A and HP3488A) through which the temperatures are automatically recorded by a computer.

Heat transfer and pressure drop experiments are carried out with three different helical tubes for the single-phase flow case. One of the tubes is the smooth helical tube, which is used to verify the experimental reliability, accuracy and benchmark the experimental results. The others for single-phase flow are 3D internally finned helical tubes. The 3D internally-finned tube used for single-phase study is a patented product, which are mechanically fabricated by using a patented special cutting tool [8]. All of these tubes have the same curvature of 0.0663 and the inner diameter of 12.0 mm. The internal surface schematic drawings of these testing tubes are shown in Fig. 4 and the geometry parameters are shown in Table 1.

For the two-phase (boiling) flow experiment, the experimental scheme is shown in Fig. 2 and the detailed experimental apparatus have been explained in reference [4]. In this experiment, the 3D micro-finned tube used for two-phase study is produced by boring and internal grooving part of the fins of commercially available 2D micro-finned tube. The geometries of the internal micro-fins is measured by cutting the tube into several sections and mapping the fin configuration and distribution into a pre-measured scale board using optical microscopic. By this way, the 3-D internal and micro fins can be accurately measured. The internal surface outline of these tubes is shown in Fig. 5 and all the geometry parameters are also shown in Table 1.
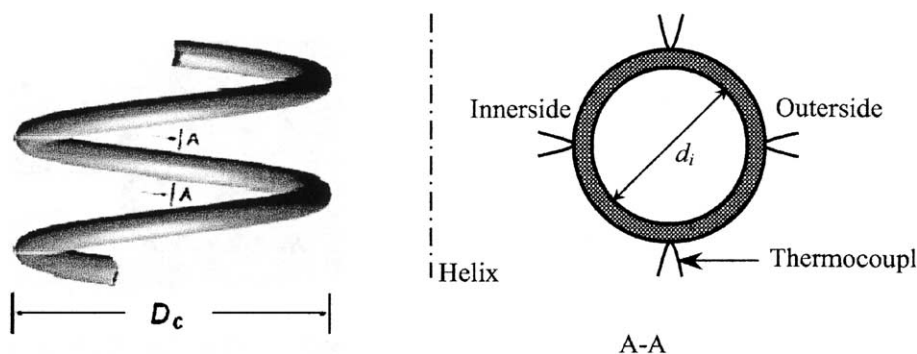

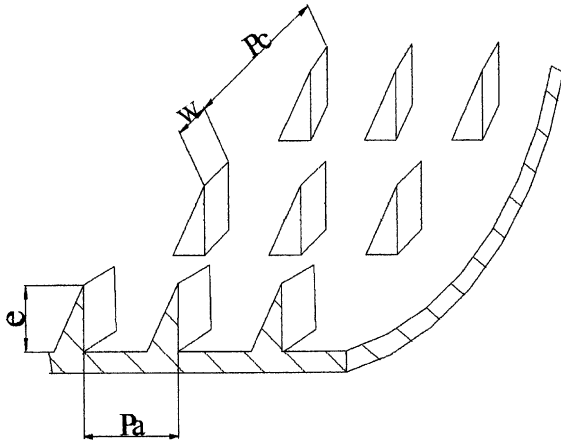Fig. 3. Schematics of the thermocouples' location.

Fig. 4. Schematics of internal surface of 3D internally-finned tube.

Fig. 5. Schematics of internal surface of 3D micro-fin tube.

The main difference between these two experimental systems is the medium cooling subsystem. In the single-phase flow system, the cooling subsystem includes just one condenser only, whose purpose is to cool the hot medium from the test section. But in the two-phase (boiling) flow experimental system, this subsystem consists of two parts: one is the vapor condenser, which condenses the vapor medium to the liquid; and the other is the liquid cooler. In general, it will take at least 30 min each time to reach the stable experimental conditions for both single- and two-phase experiments. It was considered that the stable condition is achieved when the temperature variation measured by the data acquisition system, is less than 0.1 °C.

3. Data analysis and uncertainty

The instrumental errors involved in both single-phase and two-phase (boiling) flow experiments are shown in Table 2, and the error analysis in this paper is based on the policy of reporting uncertainties in experimental measurements and results [9,10]. According to these references, the experimental uncertainty is defined as follow:
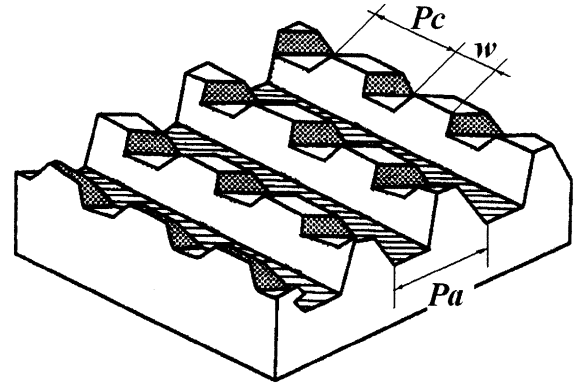
For the variable R, $R = R(x_1, x_2, x_3 \cdots x_n)$, the uncertainty is defined as,

$$U_R = \{(B_R)^2 + (P_R)^2\}^{1/2} \tag{1}$$

Where, the B_R and P_R are the bias limit and the precision limit of variable R, respectively. And they are defined as follows,

$$B_R = \left\{ \left(\frac{\partial R}{\partial x_1} Bx_1\right)^2 + \left(\frac{\partial R}{\partial x_2} Bx_2\right)^2 + \left(\frac{\partial R}{\partial x_3} Bx_3\right)^2 \cdots \right. \\ \left. + \left(\frac{\partial R}{\partial x_n} Bx_n\right)^2 \right\}^{1/2} \tag{2}$$

$$P_R = \left\{ \left(\frac{\partial R}{\partial x_1} Px_1\right)^2 + \left(\frac{\partial R}{\partial x_2} Px_2\right)^2 + \left(\frac{\partial R}{\partial x_3} Px_3\right)^2 \cdots \right. \\ \left. + \left(\frac{\partial R}{\partial x_n} Px_n\right)^2 \right\}^{1/2} \tag{3}$$

Generally, it is difficult to find the bias error for the specific experiment system because B_R is an estimate of the magnitude of the fixed, constant error. Therefore, in this paper we just consider the precision limit, P_R, and regard this error as the experimental uncertainty of the specific variable.

$$U_R = P_R \tag{4}$$

Table 1
Geometry of the 3D internal fin

Experiments	Items	d_i (mm)	D_c (mm)	δ	e (mm)	P_a (mm)	W (mm)	P_c (mm)
Single phase flow	Smooth helical tube	12.0	181.0	0.0663	–	–	–	–
	3D internal finned tube #1	12.0	181.0	0.0663	0.65	2.0	0.5	3.14
	3D internal finned tube #2	12.0	181.0	0.0663	0.95	4.0	0.5	3.14
Two phase flow	Smooth helical tube	10.0	180.0	0.0555	–	–	–	–
	3D micro-finned tube	11.2	185.0	0.0605	0.25	1.0	0.3	0.59

Table 2
Uncertainty of the instruments

Parameters	Sensor	Error
Temperature (°C)	ϕ 0.2T type thermal couple	±0.15 °C
Mass Flux (kg/h)	Flow meter	±2.0 kg/h
Pressure (kPa)	Pressure gauge	±2.0 kPa
Pressure Drop (Pa)	U type pressure gauge	±133.0 Pa
Current (A)	Ampere meter	0.1%
Voltage (V)	Voltage meter	0.1%

3.1. Single-phase flow case

For the single-phase flow, the key parameters are Re number, Nu number and the friction resistance factor. For example, the Re number is defined as:

$$Re = \frac{u \cdot d}{v} \tag{5}$$

And,

$$G = u \cdot A \cdot \rho = \frac{\pi \cdot u \cdot d^2 \cdot \rho}{4} \tag{6}$$

So, from the formula (5) and (6), we can have:

$$Re = \frac{u \cdot d}{v} = \frac{4G}{\pi \cdot d \cdot \rho \cdot v} \tag{7}$$

3.2. Two-phase (boiling) flow case

For the two-phase (boiling) flow experiment, the heat transfer coefficient and the vapor quality are defined as follows:

$$h = \frac{Q_{\text{test}}}{F \cdot (t_{w,i} - t_s)} = \frac{U \cdot I}{F \cdot (t_{w,i} - t_s)} \tag{10}$$

$$x = \frac{Q_{\text{pre}} - m \cdot C_p \cdot (t_s - t_{\text{pre}})}{m \cdot r}$$
$$= \frac{U \cdot I - m \cdot C_p \cdot (t_s - t_{\text{pre}})}{m \cdot r} \tag{11}$$

Therefore, the uncertainties for these two parameters are:

$$\frac{U_h}{h} = \frac{P_h}{h} = \sqrt{\left(\frac{P_U}{U}\right)^2 + \left(\frac{P_I}{I}\right)^2 + \left(\frac{t_{w,i}}{t_{w,i} - t_s}\right)^2 \cdot \left(\frac{P_{t_{w,i}}}{t_{w,i}}\right)^2 + \left(\frac{t_s}{t_{w,i} - t_s}\right)^2 \cdot \left(\frac{P_{t_s}}{t_s}\right)^2} \tag{12}$$

$$\frac{U_x}{x} = \frac{P_x}{x} = \frac{\sqrt{(I \cdot P_U)^2 + (U \cdot P_I)^2 + \left(\frac{U \cdot I}{m} \cdot P_m\right)^2 + (C_p \cdot m \cdot P_{t_s})^2 + (C_p \cdot m \cdot P_{t_{\text{pre}}})^2}}{U \cdot I - m \cdot C_p \cdot (t_s - t_{\text{pre}})} \tag{13}$$

According to the definition of P_R, we can get:

$$\left(\frac{P_{Re}}{Re}\right)^2 = \left(\frac{\partial Re}{\partial G} \cdot \frac{1}{Re}\right)^2 \cdot P_G^2 + \left(\frac{\partial Re}{\partial d} \cdot \frac{1}{Re}\right)^2 \cdot P_d^2 \tag{8}$$

Therefore, the uncertainty of the Re number is:

$$\frac{U_{Re}}{Re} = \frac{P_{Re}}{Re}$$
$$= \sqrt{\left(\frac{4}{\pi \cdot d \cdot \rho \cdot v \cdot Re}\right)^2 \cdot P_G^2 + \left(\frac{4G}{\pi \cdot d^2 \cdot \rho \cdot v \cdot Re}\right)^2 \cdot P_d^2} \tag{9}$$

Then, we can get the uncertainty for Re number ±2.0%, similarly for Nu number ±11.5% and friction resistance factor (f_c) ± 3.5%.

Finally, in the two-phase (boiling) flow experiment the uncertainties are for heat transfer coefficient (h) of ±10.6% and vapor quality (x) ±2.6%.

It is worth noting that the heat transfer coefficient used in the two-phase flow is the vapor quality integrated average value. The definition of this parameter is as follow:

$$\bar{h} = \frac{\int_{x_1}^{x_2} h \, dx}{x_2 - x_1} = \frac{\sum_i h_i \delta x_i}{x_2 - x_1} \tag{14}$$

4. Results and discussion

4.1. Single-phase case analyse

From the previous researches [11,12], the secondary flow was observed tending to stabilize the laminar flow

in the helical tube; therefore the critical Reynolds number for the beginning of the transition from laminar to turbulent flow in helical tube is higher than that in a straight tube. Schmidt [11] recommended that the critical Reynolds number could be calculated with the following formula:

$$Re_{crit} = 2300(1 + 8.6\delta^{0.45}) \qquad (15)$$

Where $0.0016 \leqslant \delta \leqslant 0.067$. Srinivasan et al. [12] introduced another formula to calculate the critical Reynolds number for flow in coils:

$$Re_{crit} = 2100(1 + 12\delta^{0.45}) \qquad (16)$$

where $0.009 \leqslant \delta \leqslant 0.05$.

Since the curvature of the helical tube in this research is 0.0663, the calculated critical Reynolds numbers from the above two formulations are 8133 and 8588, respectively. Also, since the flowing medium in this paper is water and the Reynolds number was kept between 1900 and 8500, the flow in this experiment is remained mostly in the laminar flow regime.

Fig. 6 shows the water's friction resistance factor vs. Re number within laminar regime and Fig. 7 shows the Nu number vs. Re number both in smooth and internally finned helical tube.

For the friction resistance factor in the smooth helical tube, it is worth noting that a larger deviation was observed at high Reynolds number in Fig. 6, because, at this time, the flow is closer to the turbulent regime and it is a sign that the transition regime of flow has begun for this experiment. Compared with the Srinivasan's results [12], the average error is 5.48% and the maximum deviation is less than ±7.0%; compared with the Manlapaz and Churchill's results [3], the average error is 4.25% and the maximum deviation is less than ±5.5%.
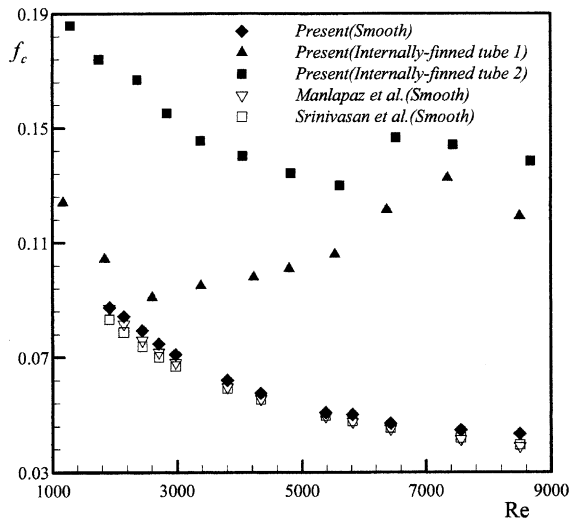

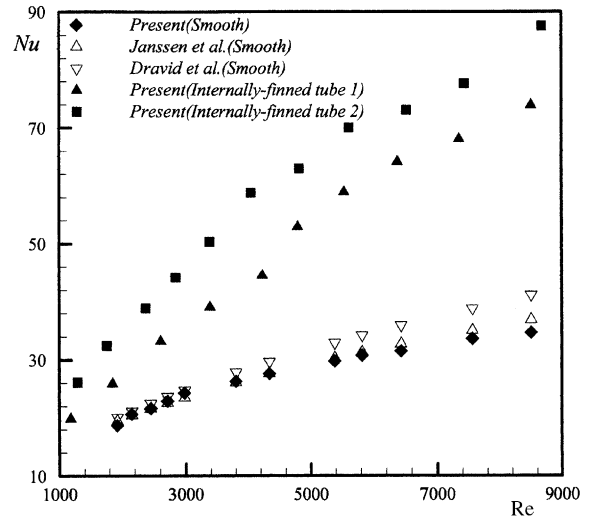Fig. 6. Flow resistance vs. Re number in single-phase flow.

Fig. 7. Nu number vs. Re number in single-phase flow.

For the heat transfer gain in the smooth helical tube, previous researchers have suggested some semi-empirical formulas from their experimental studies. Janssen and Hoogendoorn [13] introduced the following formula:

$$Nu = 0.7Re^{0.43}Pr^{1/6}\delta^{0.07}, \quad Pr > 20 \qquad (17)$$

where $0.01 \leqslant \delta \leqslant 0.083$, $Pr > 20$.

Dravid et al. [2] brought another empirical formula, which is suitable for broader conditions.

$$Nu = (0.76 + 0.65Dn^{0.5})Pr^{0.175} \qquad (18)$$

Where, $50 < Dn < 2000$ and $5 < Pr < 175$.

From Fig. 7, the calculated Nu number for the smooth helical tube from our measurements are lower by only 0.7% than that given formula of Janssen and Hoogendroorn [13], with maximum deviation less than ±4.0%. But for the formula of Dravid et al. [2], the results are lower by 6.88% with maximum deviation less than ±10.0%.

Therefore, based on the experimental data of single-phase flow and heat transfer in the smooth helical tube, it is concluded that the experimental data from this study are consistent with the previous results, then the experimental measurements and method used in this study are accurate and reliable. Hence, this experiment may so be applied to the internally finned tube cases.

For the internally finned helical tube, it can be seen in Figs. 6 and 7 that the friction factor and Nusselt number of tube 1 are lower than that of tube 2. Since tube 1 has shorter fin height, Figs. 6 and 7 conform that the less friction is associated to less heat transfer. In Fig. 7, the average heat transfer augmentation ratio of tube 1 in respect to smooth helical tube is 1.71 with a maximum up to 2.1. At the same time, the average flow resistance increase ratio of this tube is 1.9 (see Fig. 6). For the tube 2,

the average heat transfer augmentation ratio is 2.03 with a maximum up to 2.3, and the average flow resistance increase ratio is about 2.4. It is well believed that the heat transfer augmentation in a 3D structure depends on the area of heat transfer surface in the laminar flow regime. With the increase of Reynolds number, the effects of coarse surface to the flow disturbance will also be increased, resulting so in early transition from the laminar flow to turbulent flow. Although the secondary flow tends to stabilize the flow in the laminar flow regime, thus causing the critical Reynolds number reach 8500 in the smooth helical tube, the transition region may begin earlier in the presence of internal fins, which disturb the flow. In such case, the flow pattern is complex and there exist not only the effects of centrifugal and Coriolis forces on both the secondary flow and main flow, but also the disturbing effect of a finned surface. It is worth noting that this type of complex flow study has not been seen in the literature.

4.2. Two-phase flow case analysis

In this experimental investigation, the two-phase (boiling) flow heat transfer and friction resistance are measured using the commercial refrigerant R134a for both smooth helical tube and 3D internal micro-finned helical tube. The experimental conditions are as follows: pressure (P) 0.49–0.67 MPa, medium mass flow rate (G) 70.0–320.0 kg/m^2 s, heat flux (q) 2.0–22.0 kW/m^2 and the medium vapor quality (x) 0.1–0.8.

The flow pressure drop per unit length in smooth and 3D internal micro-firmed helical tube is shown in Fig. 8. In this figure, the average vapor quality of the refrigerant varies from 0.12 to 0.25 and from 0.52 to 0.64 and the flow is in the two-phase flow regime. As it can be

seen from Fig. 8, with the increase of refrigerant mass flow rate, the pressure drops in boiling flow is also increased in both smooth and 3D micro-finned helical tubes. Also, the pressure drops to the higher vapor quality flow is larger than that to the lower vapor quality flow. In addition, all of the pressure drops in 3D internal micro-finned helical tube are higher than those of the smooth one and the increasing rate in micro-finned tubes is faster than that of smooth one when the mass flow ratio is increased.

The average heat transfer coefficient obtained in 3D micro-finned tubes, which is calculated based on the vapor quality ranging from 0.1–0.8, vs. mass flow rate are shown in Fig. 9. From this figure, with the increase of mass flow rate, the average heat transfer coefficient is slightly increased. At the same time, the higher the heat flux results in the larger heat transfer coefficient. These trends are consistent with the results from straight smooth and internally finned pipes that the nucleate boiling sites are significantly increased with increased heat flux, and the bubble departing frequency increases when the mass flow rate is increased. Both effects result in heat transfer rate enhancement in the helical tubes.

The pressure drop and heat transfer augmentation ratio of 3D internal micro-finned tube to smooth helical tube vs. refrigerant mass flow rate are shown in Fig. 10. From this figure, it can be seen clearly that with the increase of mass flow rate, the relative pressure drop, which is in between 1.18 and 2.19, is also increased and has higher values for the higher vapor quality flow. At the same time, the heat transfer augmentation ratio, which is in between 1.4 and 2.2, is decreased when the mass flow rate increases, and has larger values under the lower heat flux conditions. This phenomenon
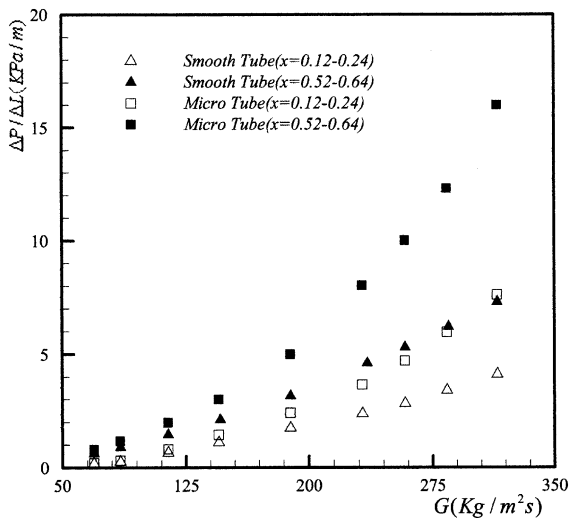

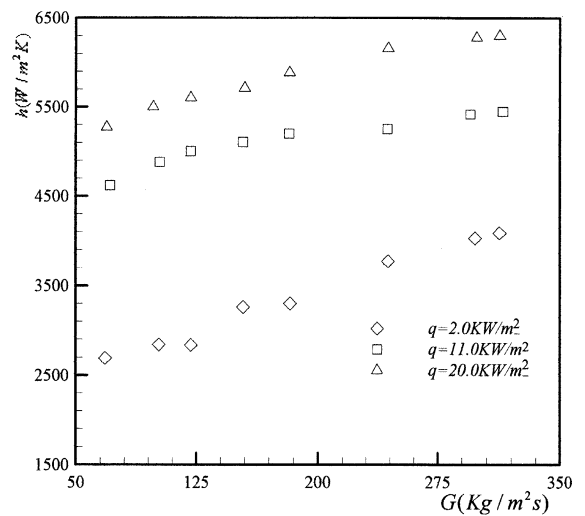Fig. 8. Pressure drops in two-phase flow.

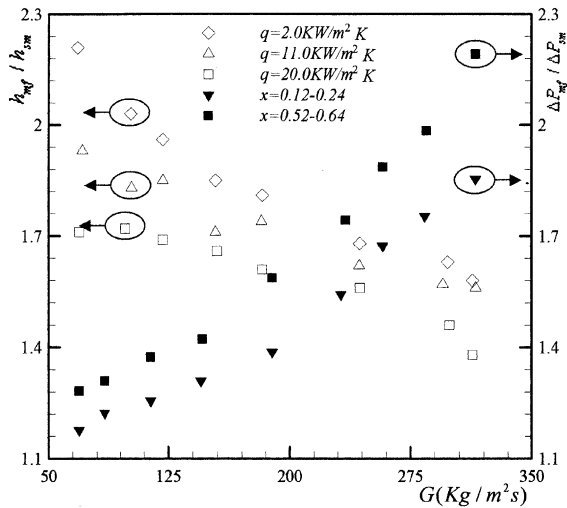Fig. 9. Average boiling heat transfer coefficients in the two-phase flow.

Fig. 10. Augmentation ratio of boiling heat transfer and pressure drop vs. mass flux in 3D micro-finned helical tube.

suggests that the higher the heat flux and/or the mass flow ratio, the less significant the heat transfer enhancement ratio. In another word, with the heat flux and/or mass flow ratio increased, the effects of the heat flux and/or mass flow rate on the heat transfer coefficient ratio of 3D micro-finned tube to smooth helical tube are decreased. This is because, by maintaining the same heat flux and increasing the mass flow rate, the boiling heat transfer on the micro-finned surface is greatly suppressed due the centrifugal and Coriolis forces acting on the internal wall. However, the convective heat transfer is slightly enhanced due to larger bubble departing frequency at larger mass flow rate. On the other hand, by maintaining the same mass flow rate and increasing the heat flux, the convective heat transfer is mildly increased. This is because the boiling nucleate sites are increased as the heat flux is increased, thus the boiling heat transfer performance is enhanced. Due to the decreasing increases in heat transfer rate when either the heat flux or mass flow rate is increased, the ratio of the overall average heat transfer coefficient (h_{mf}/h_{sm}) could not be significantly increased as shown in Fig. 10.

5. Conclusions

Experiments are performed to investigate the single-phase flow and flow-boiling heat transfer augmentation in 3D internally finned and micro-finned helical tubes.

In the single-phase flow experiment, the obtained data in smooth helical tube agrees very well with the existing experimental data. Within the applied range of Reynolds number, compared with the smooth helical tube, the average heat transfer augmentation ratio for the two finned tubes is 71% and 103%, but associated with a flow resistance increase of 90% and 140%, respectively. It is concluded that a higher fin height results in a higher heat transfer rate and a larger friction flow resistance.

Compared with that in the smooth helical tube, the boiling heat transfer coefficient in the 3D internally micro-finned helical tube is increased by 40–120% under varied mass flow rate and wall heat flux conditions, meanwhile, the flow resistance is increased by 18–119%, respectively.

From the two-phase (boiling) flow experiment, it is found that the boiling heat transfer coefficient in the 3D internally micro-finned helical tube is increased by 40–120% and the flow resistance is increased by 18–119%, respectively. It is concluded that the better heat transfer augmentation with higher fin, thus the special geometry of the 3D internal micro-fins can significantly enhance the flow boiling heat transfer in the helical tube.

References

[1] G.W. Hogg, The effect of Secondary Flow on Point Heat Transfer Coefficient for Turbulent Flow Inside Curved Tubes, Ph.D. Thesis, Univ. of Idaho., 1968.

[2] A.N. Dravid, K.A. Smith, E.W. Merrill, Effect on secondary fluid motion of a curved tube, AICHE J 17 (1971) 1114–1122.

[3] R.L. Manlapaz, S.W. Churchill, Fully developed laminar flow in a helically coiled tube of finite pitch, Chem. Eng. Commun. 7 (1980) 57–78.

[4] W. Cui, Q. Liao, M. Xin, Flow boiling heat transfer of R134a in heliacally coiled tube, J. Chongqing University 24 (4) (2001) 118–121.

[5] G. Liao, C. Gao, C. Wang, Experimental study on flow and heat transfer in 3D internal fined tube, J. Eng. Thermophys. 11 (4) (1990) 386–392.

[6] A.E. Bergles, Heat transfer enhancement—the maturing of second-generation heat transfer technology, Heat Transfer Eng. 18 (1) (1997) 47–55.

[7] L.M. Chamra, R.L. Webb, Advanced micro-fin tubes for evaporation, Int. J. Heat Mass Transfer 39 (9) (1996) 1827–1838.

[8] G.Y. Liao, Three Dimensional internally Fined Tube and the Fabricated Technics, China Patent no: 88102575.5, 1988.

[9] J.H. Kim, T.W. Simon, R. Viskanta, Journal of Heat Transfer policy on reporting uncertainties in experimental

measurements and results (Editorial), J. Heat Transfer 115 (l) (1993) 5–6.

[10] R.J. Moffat, Using uncertainty analysis in the planning of an experiment, ASME J. Fluids Eng. 107 (2) (1985) 173–178.

[11] E.F. Schmidt, Warmeubergang und druckverlust in Rohrschlangen, Chemie- Ing.-Techn. 36 (1967) 781–789.

[12] P.S. Srinivsan, S.S. Nandapurkar, F.A. Holland, Friction factors for coils, Tram. Inst. Chem. Eng. 48 (1970) T156–T161.

[13] L.A.M. Jassen, C.J. Hoogendoorn, Laminar convective heat transfer in helical coiled tubes, Int. J. Heat Mass Transfer 21 (1978) 1197–1206.